Journal of Geodesy (2002) 76: 247–258
DOI 10.1007/s00190-001-0242-5

Journal of Geodesy



# Prediction of Earth orientation parameters by artificial neural networks

**H. Schuh[1], M. Ulrich[2], D. Egger[3], J. Müller[4], W. Schwegmann[5]**

[1] Institut für Geodäsie und Geophysik, Technische Universität Wien, Gusshausstrasse 27–29, 1040 Wien, Austria
e-mail: hschuh@luna.tuwien.ac.at; Tel.: +43-1-58801-12860; Fax: +43-1-58801-12896
[2] Lehrstuhl für Photogrammetrie und Fernerkundung, Technische Universität München, Arcisstrasse 21, 80290 München, Germany
e-mail: markus.ulrich@bv.tum.de; Tel.: +49-89-289-22643; Fax: +49-89-280-9573
[3] Forschungseinrichtung Satellitengeodäsie, Technische Universität München, Arcisstrasse 21, 80333 München, Germany
e-mail: dieter.egger@bv.tum.de; Tel.: +49-89-289-23183; Fax: +49-89-289-23178
[4] Institut für Astronomische und Physikalische Geodäsie, Technische Universität München, Arcisstrasse 21, 80333 München, Germany.
Now at: Universität Hannover, Institut für Erdmessung, Schneiderberg 50, 30167 Hannover, Germany
e-mail: mueller@ife.uni-hannover.de; Tel.: +49 (0)511/762-3362; Fax: +49 (0)511/762-4068; http://www.ife.uni-hannover.de
[5] CNR Istituto Di Radioastronomia, Via P. Gobetti, 101, 40129 Bologna, Italy
e-mail: schwegma@ira.bo.cnr.it; Tel.: +39-051-6399383; Fax: +39-051-6399431

Received: 6 February 2001 / Accepted: 23 October 2001

**Abstract.** Earth orientation parameters (EOPs) [polar motion and length of day (LOD), or UT1–UTC] were predicted by artificial neural networks. EOP series from various sources, e.g. the C04 series from the International Earth Rotation Service and the re-analysis optical astrometry series based on the HIPPARCOS frame, served for training the neural network for both short-term and long-term predictions. At first, all effects which can be described by functional models, e.g. effects of the solid Earth tides and the ocean tides or seasonal atmospheric variations of the EOPs, were removed. Only the differences between the modeled and the observed EOPs, i.e. the quasi-periodic and irregular variations, were used for training and prediction. The Stuttgart neural network simulator, which is a very powerful software tool developed at the University of Stuttgart, was applied to construct and to validate different types of neural networks in order to find the optimal topology of the net, the most economical learning algorithm and the best procedure to feed the net with data patterns. The results of the prediction were analyzed and compared with those obtained by other methods. The accuracy of the prediction is equal to or even better than that by other prediction methods.

**Keywords:** Earth Rotation – Prediction – Neural Networks

*Correspondence to:* H. Schuh

## 1 Introduction

The development of high-precision space-geodetic techniques during the last two decades has enabled the Earth orientation parameters (EOPs) to be observed with steadily increasing accuracy. Their exact knowledge is important for many investigations in geodesy and astronomy. There is a growing demand for the availability of precise EOPs in real time. Real-time values of EOPs are needed for various applications, e.g. for high-precision terrestrial navigation by use of the global positioning system (GPS), for the navigation of Earth satellites and interplanetary spacecrafts, and for laser ranging to satellites and to the Moon. However, the precise measurements of EOPs by space-geodetic techniques have to be pre-processed before the EOPs are available. This causes a delay of 15 to 20 hours in the case of GPS and of a few days in case of very-long-baseline interferometry (VLBI) and satellite laser ranging (SLR). The latter techniques are essential for stabilizing the GPS results to avoid systematic effects, which could influence the short-term prediction too. Thus, it is necessary to predict the EOPs at least over a few days. In addition, it might be interesting to look further into the future to estimate the Earth's rotation in the next few months, years, or even decades. Therefore, this paper deals with short-term predictions for the next 40 days, mean-term predictions, which cover 1 year, and finally a 40-year long-term prediction of polar motion.

Predicted values of EOPs are published by several national and international services, e.g. the IERS (International Earth Rotation Service) Rapid Service/

Prediction Product Center or the EOP Service of the Institute for Astronomy and Astrophysics (IAA) in Saint Petersburg. Various prediction methods have been developed, for example by Zhu (1981, 1982), Chao (1984), McCarthy and Luzum (1991), Freedman et al. (1994), Malkin and Skurikhina (1996) and McCarthy (1996). In these methods either the parameters of harmonical functions including bias and drift are estimated and are extrapolated into the future, or stochastical tools are used, e.g. ARIMA (auto-regressive integrated moving average).

Artificial neural networks (NN) have already been successfully applied for pattern recognition, e.g. within robots or for the prediction of stock prices. The prediction of EOPs by especially designed artificial NN was examined first by Egger (1992). The comparison with a purely analytical approach which had been realized by Fröehlich revealed good agreement of the EOP predictions and showed the high potential of NN for predicting quasi-periodic and irregular processes (Egger and Fröhlich 1993).

## 2 Artificial neural networks

The human brain as the biological model for artificial NN consists of about $10^{11}$ nerve cells, which are called neurons. Each of these neurons is connected by nerve fibres with approximately 10 000 neighboring cells (Zell 1994). A neuron can be compared with a simple processing unit, which receives an input, processes it and transmits an output to the following neuron. Neurons get their inputs from predecessor cells by electro-chemical impulses, which are amplified or weakened by so-called synapses. If the sum of inputs reaching the cell body exceeds a certain threshold the neuron becomes active and sends an output to its successor cells. To describe this functionality mathematically, the biological model has to be simplified. Figure 1 shows two connected neurons $i$ and $j$. The net input *net* stands for the sum of electro-chemical impulses that arrive at the cell, the variable $a$ describes the activation of the cell and $o$ corresponds to its output. The amplifying or weakening function of the synapses is realized by a connection weight factor $w$. The calculation of the cell output $o$ can be split into three steps (Zell 1994) as follows.

1. The net input $\mathrm{net}_j$ of the cell $j$ is determined by the sum of outputs $o_i$ of all predecessor cells, each of them multiplied by the corresponding connection weight $w_{ij}$

$$\mathrm{net}_j(t) = \sum_i o_i(t) w_{ij} \tag{1}$$

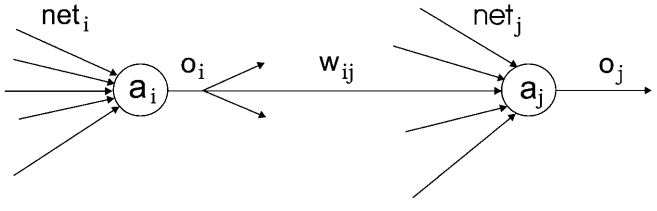


**Fig. 1.** Connection of two neurons

2. The activation $a_j\,(t+1)$ of the neuron is a function of the net input and a threshold value and thus corresponds to the threshold activity of the cell body.

$$a_j(t+1) = f_{\mathrm{act}}(\mathrm{net}_j(t), \theta_j) \tag{2}$$

The function $f_{\mathrm{act}}$ is called the activation function. In the most trivial case it is a binary function, which delivers an output 1 if the threshold is exceeded and 0 otherwise. In order to obtain continuity a sigmoidal function is usually used, e.g. the tangens hyperbolicus or the logistic function.

3. In the last step the output $o_j$ is computed as a function of the cell activation $a_j$

$$o_j = f_{\mathrm{out}}(a_j) \tag{3}$$

Generally $f_{\mathrm{out}}$ is the identity function, which means that $o_j = a_j$, as a non-linear problem is already represented by a non-linear activation function.

In most cases artificial NN consist of more than two neurons. The neurons can be connected in different ways. They are arranged in layers to approximate the biological model. Layered structures also allow the analyst to keep control when dealing with huge networks.

Figure 2 shows some examples of how neurons can be combined. In a *feedforward net* the direction of the

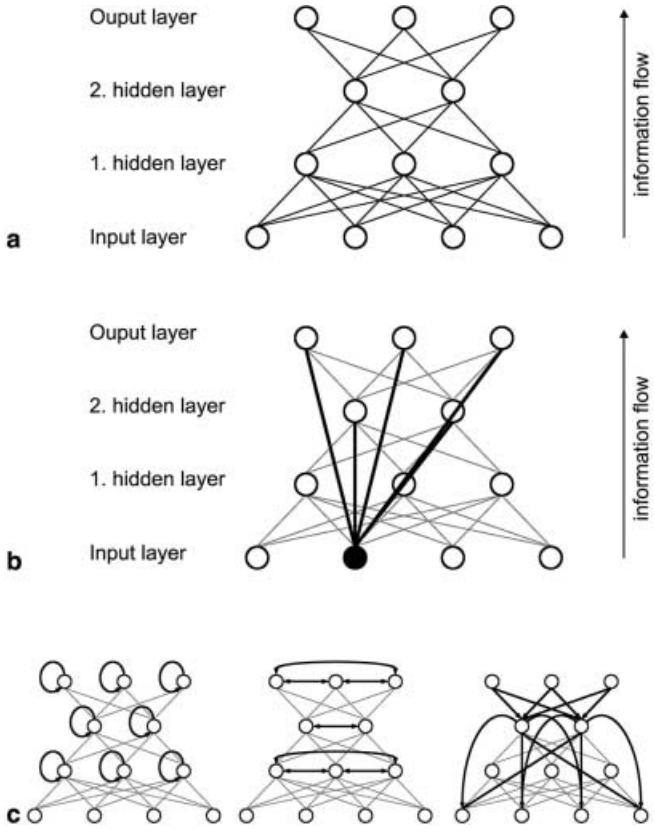


**Fig. 2a–c.** Examples of the topology of neural nets and of connections between the neurons. **a** Feedforward net with full connection; **b** feedforward net with shortcut connection; **c** feedback nets

information flow is from the *input layer* to the *output layer*. Between these two layers there can be one or more *hidden layers*. The input information is entered at the neurons of the input layer and the requested information is taken from the neurons of the output layer.

In Fig. 2a the neurons are fully connected, i.e. all neurons of a certain layer are linked with all neurons of the next and the previous layers. An example of a shortcut connection is given in Fig. 2b. Here, the black-colored neuron is directly connected with the neurons in any higher layer.

In feedback nets, which are represented in Fig. 2c, the output of one cell can be either the input of the same cell or of a neuron of the same or a lower layer. Several tests using feedback nets showed that they perform no better or even worse in the case of prediction in comparison to feedforward nets. Thus, for our purpose, i.e. a prediction of EOPs, only feedforward nets were used.

The knowledge of the net is stored in connection weights. The net has to be trained in order to find the optimal values of the connection weights. In the case of feedforward networks this is mostly done by the so-called *back-propagation* learning function. A detailed description of that algorithm can be found, for example, in Zell (1994). Here the basic procedure is explained.

1. Form a training pattern set which consists of input values and their corresponding (known) output values.
2. Initialize the connection weights with random values.
3. Choose a training input pattern out of the set and calculate the output of the net with Eqs. 1, 2, and 3 as described in the example above.
4. Compare the actual output with the output values of the training pattern set and compute the output error as the difference of the two values.
5. This error is used in the back-propagation learning formula to correct all connection weights in the net, starting with the output layer and going back to the input layer.
6. Go back to step 3 until the output error of the net is below a given threshold.

## 3 Predicting Earth orientation by artificial neural networks

The Stuttgart neural network simulator (SNNS), a very powerful piece of NN software, was used for predicting the EOPs. SNNS has been developed at the Institute for Parallel and Distributed High Performance Systems at the University of Stuttgart, Germany, since 1989 (Zell et al. 1995). It is available from a number of different sources, e.g. via anonymous ftp (ftp.informatik.uni-tuebingen.de), or as part of various LINUX distributions.

For the prediction of EOPs in terms of polar motion and length of day (LOD) or UT1–UTC a procedure was applied as described in the flowchart of Fig. 3. The observed EOP can be split up into a first part, which is rather well known because a functional model exists,

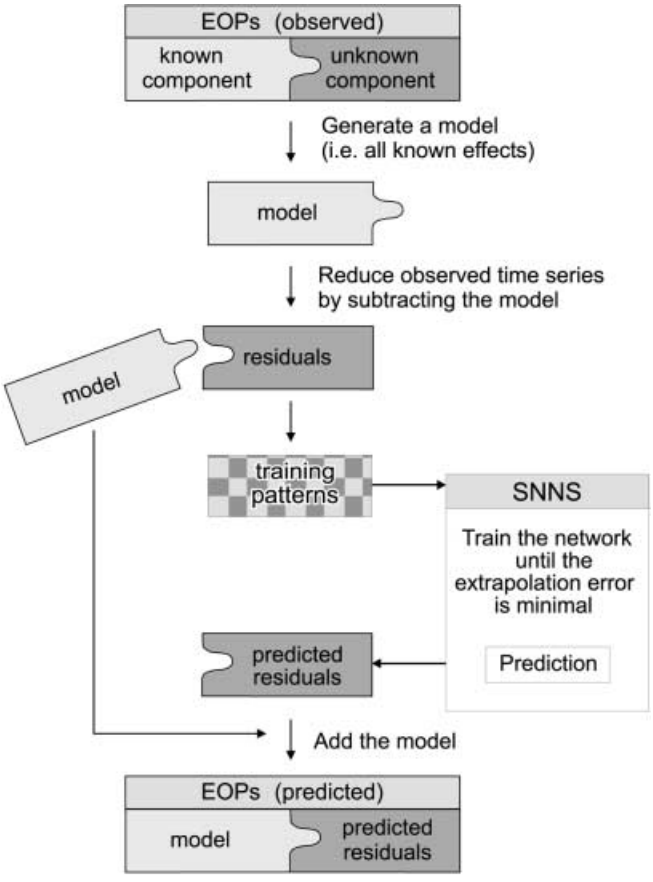


**Fig. 3.** The neural network approach for EOP prediction

and a second, unknown stochastic part. The known component, further called the *a priori model*, consists of periodic effects such as influences of the solid Earth tides and the ocean tides on the EOPs and seasonal variations. The a priori model of polar motion additionally contains the Chandler Wobble (CW). After reduction of the observed time series by subtracting the a priori model, training patterns were formed out of the residuals. These patterns were used for training the NN until the extrapolation error became a minimum. The subsequently predicted residuals were then added to the a priori model in order to obtain the predicted values of the EOPs.

In the following part of this paper the generation of the a priori models, building of the training patterns, training of the network and the net topologies used are explained. A more detailed description of this approach is given in Ulrich (2000).

### *3.1 Generation of the a priori models*

The model of LOD or UT1–UTC contains several well-known components, for example the effect of zonal Earth tides with periods from 5 days up to 18.6 years (Yoder et al. 1981). For completeness, parameters of a linear part plus seasonal variations were estimated from the observations: bias and drift of the linear part,

amplitudes ($A_a$, $A_{sa}$), frequencies ($f_a$, $f_{sa}$) and phases ($\Phi_a$, $\Phi_{sa}$) of the annual and semi-annual oscillations. The a priori model can hence be written as

$$\begin{aligned}\text{model}(t) = {} & a_0 + a_1 t + A_a \sin(2\pi f_a t + \Phi_a) \\ & + A_{sa} \sin(2\pi f_{sa} t + \Phi_{sa}) \\ & + \text{tidal terms} \end{aligned} \quad (4)$$

The stepwise reduction of LOD in the frequency domain using the IERS C04 series is shown in Fig. 4. The peaks of the residuals [bottom plot (e)] are small in comparison with the original LOD spectrum [top plot (a)]. This shows that the a priori model represents the original time series rather well.

Polar motion is essentially not influenced by zonal Earth tides. Therefore, only parameters of the linear part, i.e. bias and drift, and parameters of the annual wobble and the Chandler Wobble were estimated and introduced in the a priori model. In Fig. 5 the observed polar motion and its representation by the a priori model are plotted. The differences were used for training the artificial NN.

### *3.2 Generation of training patterns*

Next a neural net had to be designed to provide predictions of a time series such as the EOPs. As described in Sect. 2, the net needs an input before it is able to generate an output.

A first possibility is to use the variable time $t$ as the only input for feeding the net. The residuals of the EOPs at the time $t$ could then be used to form the output of the net. Such a neural net would therefore get one input and one output layer with only one neuron each. Indeed, practical experiments have shown that this method can represent the training patterns rather well, but predictions nevertheless fail. This happens because the input

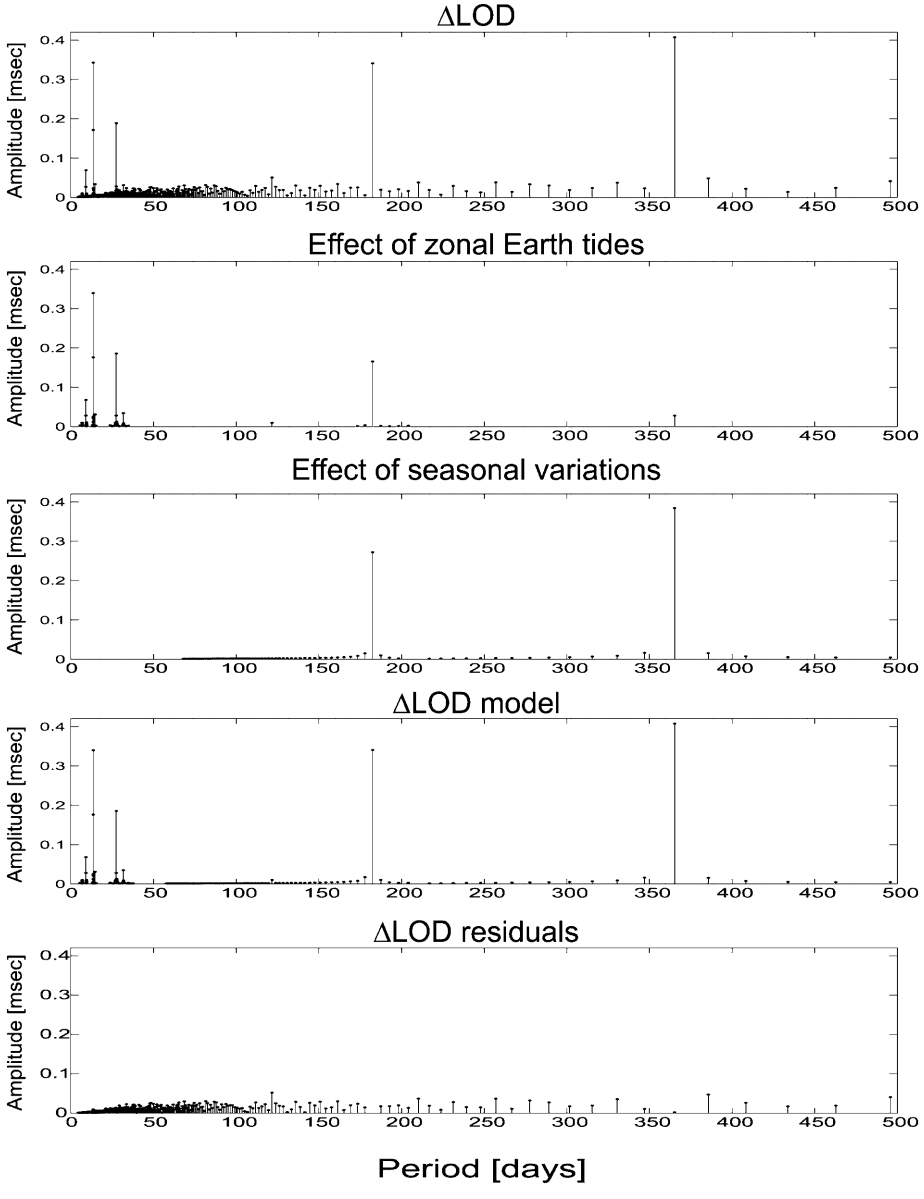


**Fig. 4a–e.** Reduction of LOD in the frequency domain: plot **a** shows the Fourier spectrum of the observed LOD values; **b** represents the effect of the zonal Earth tides using the model by Yoder et al. (1981); **c** represents the effect of the seasonal variations including annual and semi-annual oscillation; **d** as sum of **b** and **c** forms the a priori model of LOD; and **e** shows the spectrum of the LOD residuals computed as the difference between **a** and **d**

time $t$ in the case of prediction has to be extrapolated into the future. Since the values of the input data in the case of prediction, i.e. the extrapolated variable $t$, are not covered by the training data, the neural net yields poor predictions.

A more sophisticated method is to use past values as input of the net and future values as output. Figure 6 illustrates this procedure. In this example the residual EOPs of the last 1, 2, 3, 4, 5, and 8 days are used to obtain the residuals of the next 1, 2, 3, and 5 days. This pattern matrix can now be shifted along the whole time series of residual EOPs, forming a multitude of pattern pairs.

### *3.3 Training the network*

Patterns generated as described in the previous paragraph were used to train the network. It is very important, however, not to enter all the patterns during

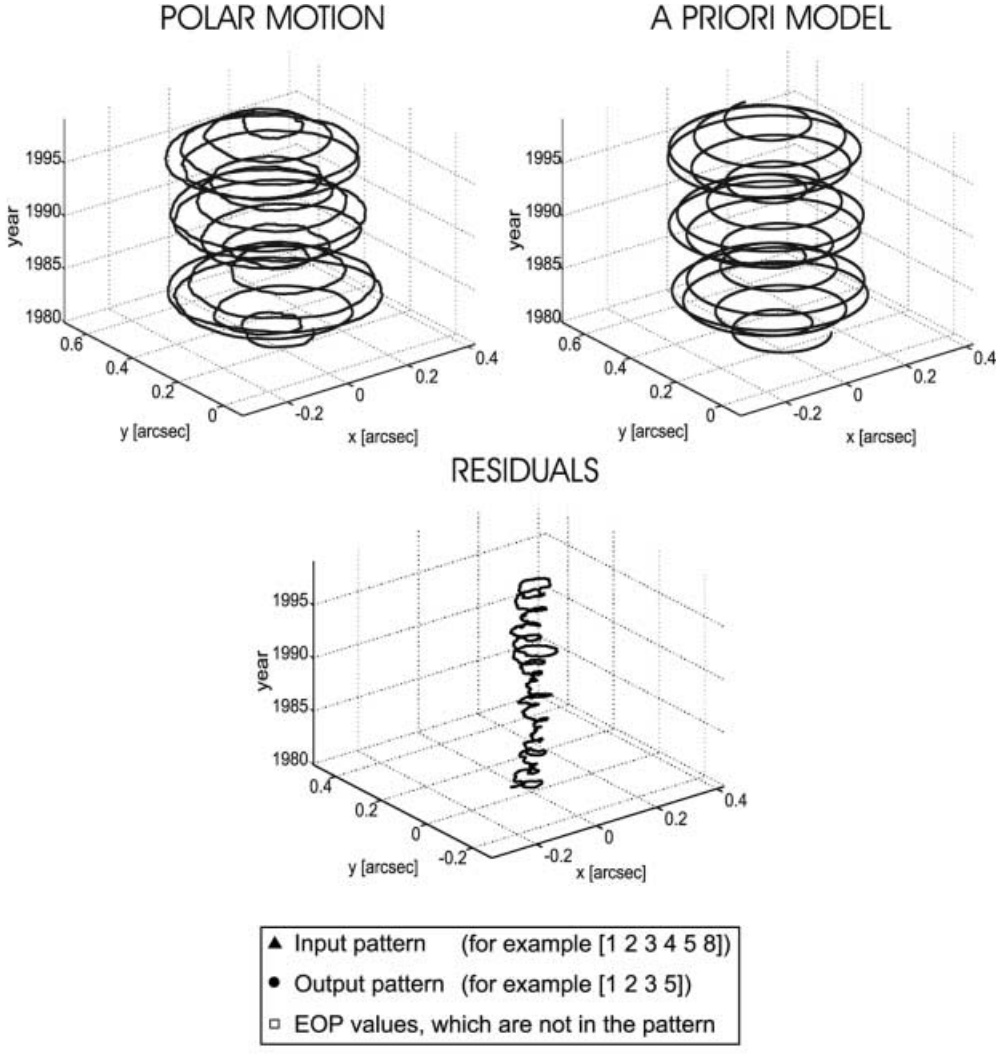


**Fig. 5.** Reduction of polar motion: the a priori model of polar motion in the upper-right plot is subtracted from the observed values shown in the upper-left plot. The differences are represented in the bottom plot

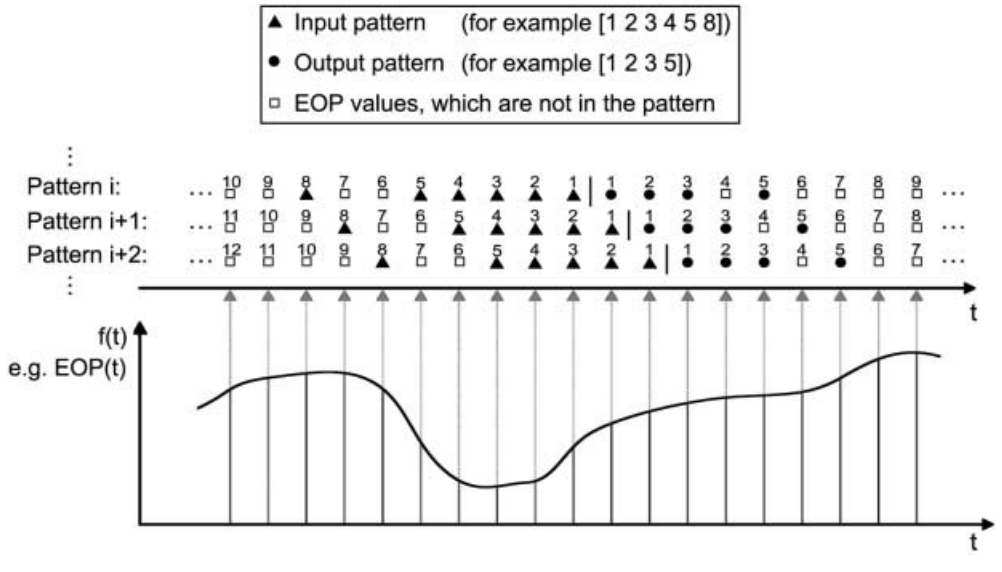


**Fig. 6.** Pattern generation

the training. Figure 7 demonstrates the principle of how the patterns were split up. The chronologically first 10% of the patterns were split off and used to form the TEST set, the central 80% represent the TRAIN set and the last 10% shape the VALID set. Only the patterns in the TRAIN set were used for training the network. The advantage of building a TEST set and a VALID set will be explained later. After every training cycle, i.e. after all training patterns of the TRAIN set had been entered once into the net, the root-mean-square (RMS) errors of the three pattern sets were computed.

A typical example of a training run is plotted in Fig. 8. As expected, the error of the TRAIN set (*black*) is getting smaller with increasing number of training cycles. In comparison, the errors of the TEST (*light gray*) and VALID (*dark gray*) sets reach their minima after a certain number of cycles. If the net is trained further, the latter errors begin to increase again and the neural net loses its ability to generalize and consequently to predict. In order to explain this characteristic, we can imagine that the net learns the noise in the training patterns too. Over-training of the net can be avoided if the training is stopped at the minimum of the prediction error, i.e. when the error of the VALID set becomes a minimum. In practice, there is no way to validate the prediction of the net. Therefore, we generated the TEST set, which can be interpreted as a 'prediction' into the past. For this set we were able to compute the RMS error very well and therefore we obtained a criterion for when the training had to be stopped. In general, the minima of the TEST and the VALID sets are not reached after the same number of training cycles, but this method represents an acceptable compromise to avoid over-training of the net.

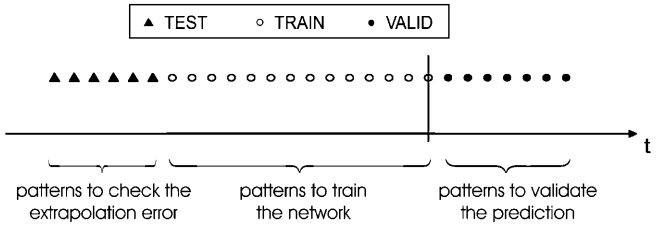


**Fig. 7.** The three pattern sets, which are shifted along the time series during the training phase of the neural network

### *3.4 Topology of the net*

It can be difficult to find the optimal topology of a neural net used for a special task.

The number of input and output neurons of the network has to be chosen and the optimal quantity of hidden layers and neurons per layer has to be found. As there are only some general remarks and hints in the literature (e.g. Cybenko 1989; Conway 1998), trials and tests are still necessary.

On the one hand, the number of neurons should not be too big because otherwise the training would take too much time. On the other hand, too few neurons would allow only a poor representation of the a priori time series. Therefore, a compromise has to be found.

Feedforward nets turned out to be superior to feedback networks for our applications. For example, we used a feedforward net with 17 input neurons, two hidden layers with eight and four neurons respectively, and 12 output neurons for mean-term prediction up to 1 year. The input information contains EOP values of the last 1260 days which are distributed over 16 input neurons in a way that the interval between two neurons (measured in days) gets bigger the further the EOP values lie in the past because the recent data are more important for prediction than the older data. The 12 output neurons correspond to prediction values with equidistant intervals of 30 days each.

Standard back-propagation with a logistic activation function was used to train the net. When training the patterns in chronological order the decrease of the RMS errors became slow or it even stagnated. The training time could be shortened considerably by representing the patterns during the training in random order.

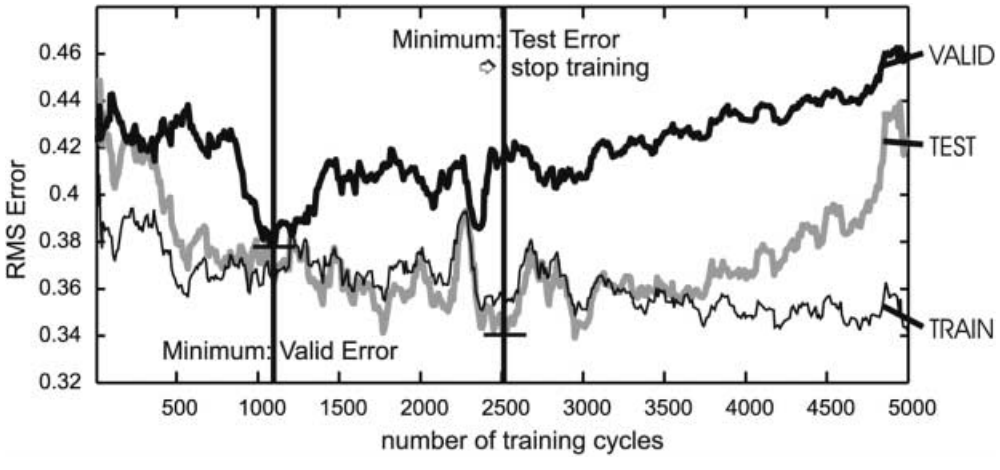


**Fig. 8.** RMS errors during the training

## 4 Examples

Figure 9a shows a 1-year prediction of LOD starting in March 2000. The neural net was trained with LOD values of IERS C04 series from 1980 until February 2000. Figure 9b shows the corresponding prediction error using the C04 series as reference, i.e. the differences between the predicted LOD values of the neural net and the actual values taken from the C04 series are plotted. As can be seen, in the whole prediction time range of 1 year the error does not exceed 0.6 msec. The mean value of the absolute prediction errors is 0.21 msec.

A remarkable phenomenon can be seen in Fig. 10, which shows the results of the predictions 10 days into the future (*solid line*) and the C04 series reduced by the a priori model (*dotted line*). During the training period, which lasted from 1980 until 1997, there was an extraordinary peak due to a strong El Niño event in 1983. The characteristic behavior before the 1983 El Niño was apparently stored in the input patterns and, in February 1998, when there was another El Niño, its effect was clearly predicted at the right time. However, the magnitude of this peak was predicted too large, since the 1998 El Niño was less intense than that of 1983.

In Figs. 11a and 12a a comparison is given between the 1-year prediction of polar motion and the prediction made by the IERS Rapid Service/Prediction Product Center. Additionally, the true polar motion values, which are given in the C04 series, are plotted. In order to validate the prediction, Figs. 11b and 12b show the differences between the predicted polar motion components and the values of the C04 series. In these prediction examples the IERS prediction performs better during the first half of the prediction time span, whereas the neural network is obviously superior in the second half of the prediction time span. Again, we computed the absolute prediction errors averaged over the prediction time span of 1 year to compare the quality of the predictions. For the prediction of the $x$-component of polar motion we obtained an average error of 13 marcsec when using the IERS prediction and an average error of 14 marcsec when using the prediction of the neural network. Analyzing the prediction of the $y$-component, for both approaches we obtained an average error of 15 marcsec.

An example for a long-term prediction is given in Fig. 13, which represents polar motion predicted 40 years into the future. The prediction starts in 1992 on the basis of the recomputed optical astrometry series based on the HIPPARCOS frame by Vondrák (1999). The complete observational span from 1899.7 until 1992.0 was used to train the neural net. For the long-term prediction we did not subtract a priori either the annual oscillation or the Chandler Wobble because they cannot be assumed to be constant over the next 40 years.

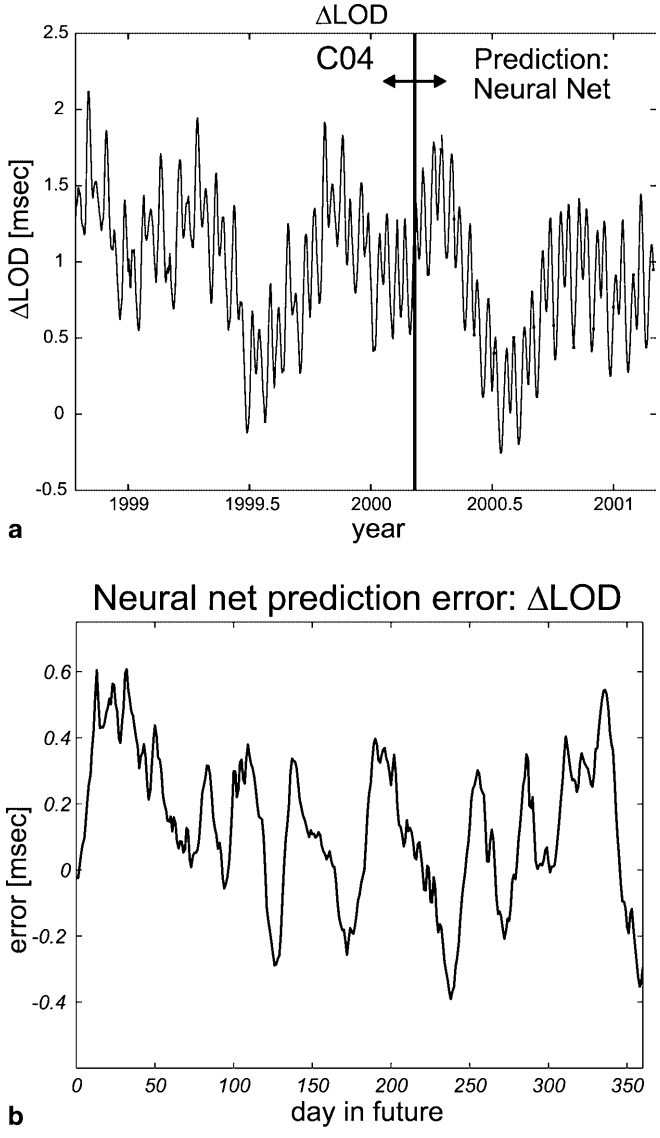


**Fig. 9a, b.** Prediction of LOD. **a** One-year prediction of LOD; **b** neural net prediction error of LOD using the C04 series as reference

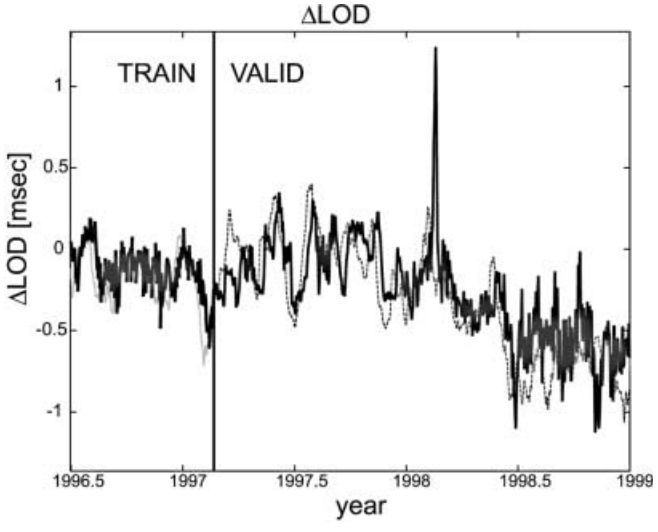


**Fig. 10.** LOD prediction (*solid line*) compared with the C04 series (*dashed line*). The striking peak in the prediction in 1998 is due to El Niño

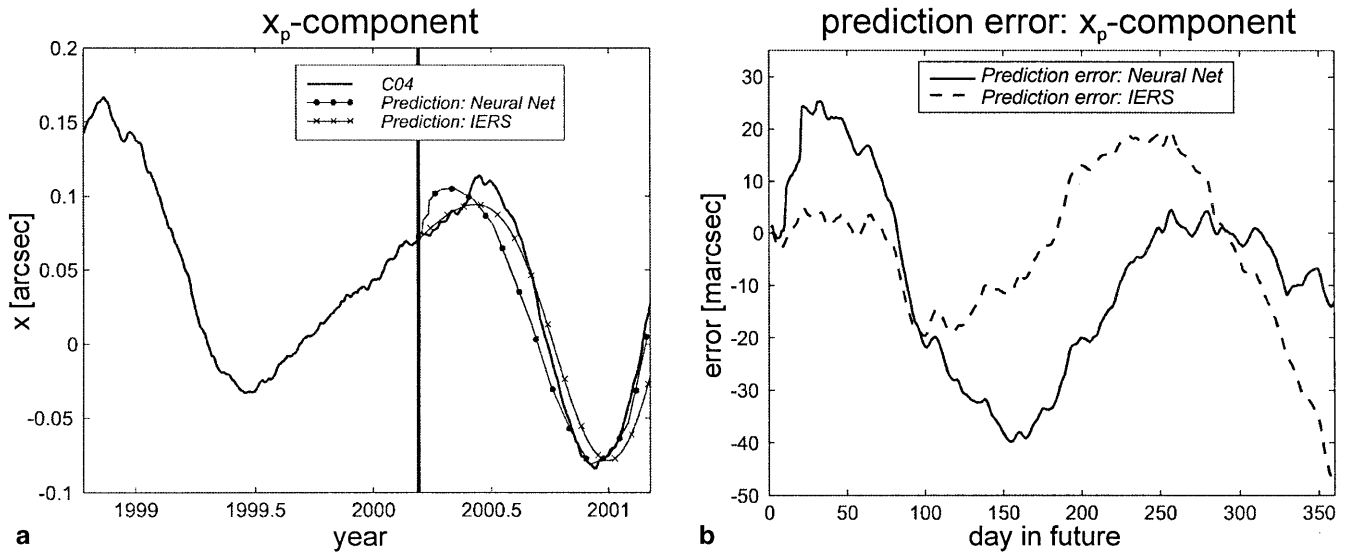


**Fig. 11a, b.** Prediction of polar motion ($x$-component). **a** One-year prediction of the $x$-component of polar motion; **b** prediction error of the $x$-component of polar motion using the C04 series as reference

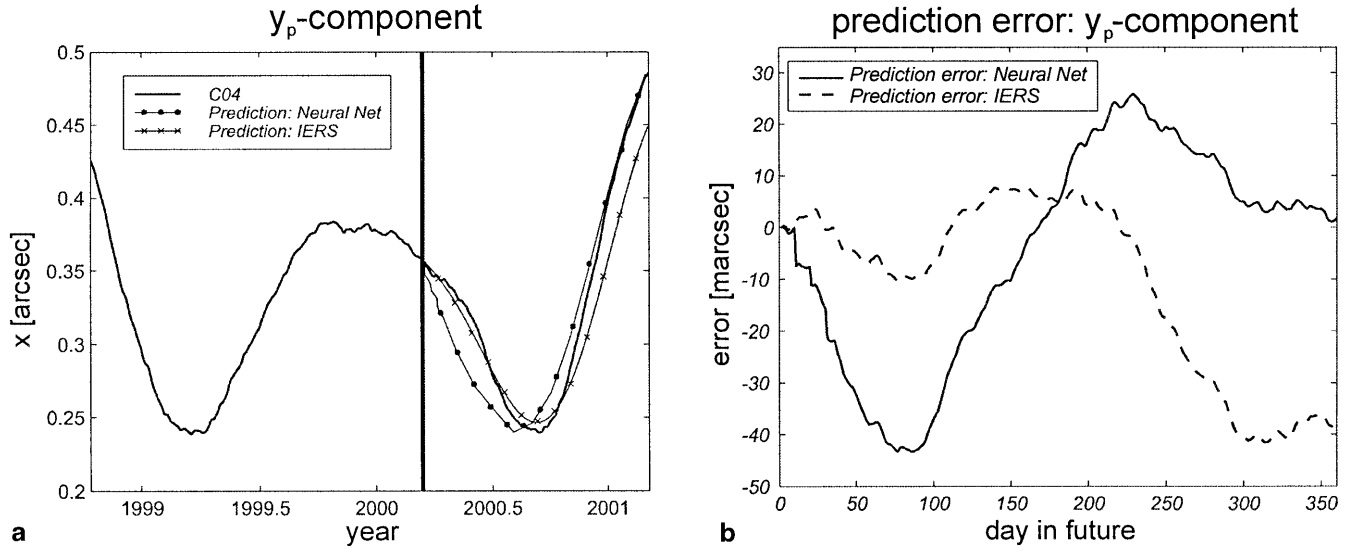


**Fig. 12a, b.** Prediction of polar motion ($y$-component). **a** one-year prediction of the $y$-component of polar motion; **b** Prediction error of the $y$-component of polar motion using the C04 series as reference

It is the task of the net to predict also those variations. Thus, the model only consists of bias and drift of $x_p$ and $y_p$. In order to validate the first 8 years of prediction, the C04 series is plotted until the year 2000. The comparison shows that phase and frequency of polar motion were predicted very well considering the long prediction interval of 40 years, whereas the predicted amplitudes differ from the observed values between 1992 and 2000. An average absolute prediction error of 32 marcsec shows the high quality of the prediction over the first 8 years.

## 5 Prediction errors and comparison with other methods

The RMS errors for different prediction intervals are summarized in Table 1. The RMS error of the prediction day $d$ was calculated by

$$\mathrm{RMS}_d = \sqrt{\frac{1}{n}\sum_{i=1}^{n}\left(p_d^i - o_d\right)^2} \tag{5}$$

with $p$ the predicted value of the artificial neural net obtained for day $d$, $o$ the real observed value of the IERS

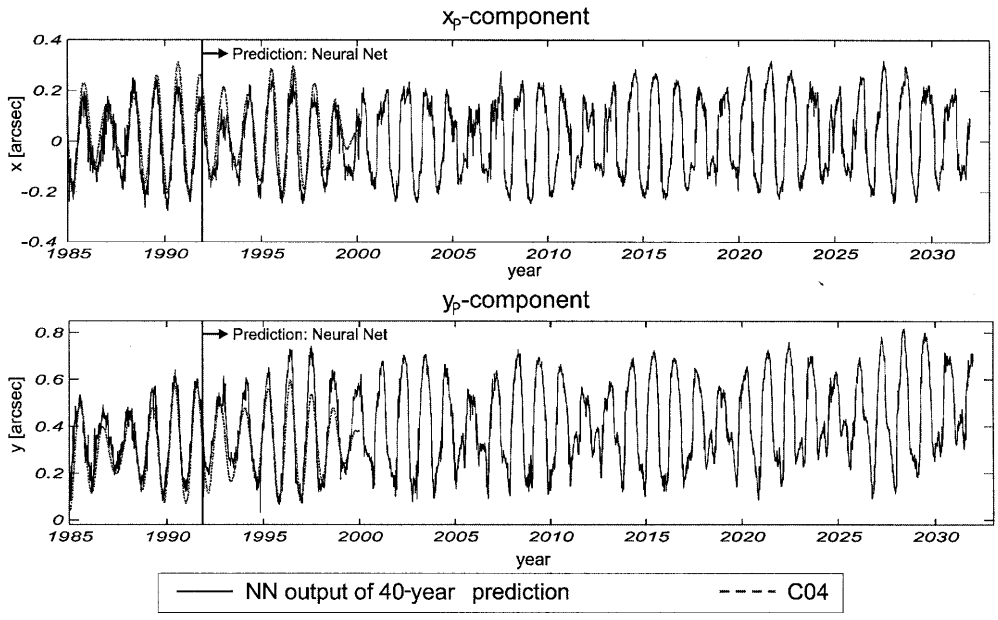


**Fig. 13.** Long-term prediction of polar motion

**Table 1.** Obtained RMS errors for different prediction intervals of polar motion, UT1–UTC and LOD

| Prediction day | $RMS^{pm}$ [marcsec] | $RMS^{UT1-UTC}$ [msec] | $RMS^{LOD}$ [msec/day] |
|---|---|---|---|
| 1 | 0.29 | 0.13 | 0.019 |
| 2 | 0.57 | 0.19 | 0.049 |
| 3 | 0.95 | 0.27 | 0.074 |
| 4 | 1.30 | 0.35 | 0.097 |
| 5 | 1.79 | 0.41 | 0.121 |
| 6 | 2.10 | 0.57 | 0.142 |
| 7 | 2.39 | 0.67 | 0.159 |
| 8 | 2.67 | 0.80 | 0.174 |
| 9 | 2.95 | 0.93 | 0.184 |
| 10 | 3.25 | 1.07 | 0.193 |
| 15 | 4.70 | 2.02 | 0.246 |
| 20 | 6.28 | 2.75 | 0.251 |
| 25 | 7.78 | 3.62 | 0.249 |
| 30 | 8.89 | 4.47 | 0.245 |
| 35 | 10.14 | 4.86 | 0.263 |
| 40 | 10.96 | 5.48 | 0.258 |
| 60 | 13.16 | 11.14 | 0.292 |
| 90 | 18.21 | 14.91 | 0.306 |
| 120 | 21.93 | 16.98 | 0.314 |
| 150 | 22.92 | 16.21 | 0.330 |
| 180 | 23.67 | 15.27 | 0.361 |
| 210 | 24.14 | 15.10 | 0.397 |
| 240 | 25.30 | 17.26 | 0.377 |
| 270 | 24.51 | 19.42 | 0.386 |
| 300 | 24.27 | 20.69 | 0.402 |
| 330 | 23.36 | 21.50 | 0.372 |
| 360 | 25.09 | 22.94 | 0.347 |

C04 series, and $n$ the number of predictions made for the particular prediction day. The corresponding NN were trained using the C04 data from 1980 until 1998. Approximately 700 predictions – starting at different days – were made for each prediction day to calculate the RMS error, i.e. $n = 700$.

A comparison with other prediction methods is given in Figs. 14–17. The references of the other prediction methods were published between 1982 and 2000. Consequently, the RMS errors given there were obtained by testing the prediction methods over different observational spans. In spite of using the same equation for computing the RMS error and the same EOP reference series (C04 of the IERS), this might have influenced the results of the other authors. A final picture of the performance of different prediction methods could only be obtained by a kind of contest where prediction period and validation strategy are clearly specified in advance. What can be said with the information available from the references is that the accuracy of NN prediction of polar motion (Figs. 14 and 15) is equal to the best prediction method found in the literature developed by Malkin and Skurikhina (1996). The RMS errors given by Chao (1984) are averaged values, i.e. the value of the $n$th prediction day represents the mean value of the prediction days 1 to $n$. Therefore, it is not directly comparable with the other methods.

In Fig. 16 it can be seen that for short-term prediction of UT1–UTC an accuracy is obtained which is equal to the best presently available prediction method. Mean-term prediction beyond 100 days (Fig. 17) is substantially better than the results of other methods.

## 6 Conclusion and outlook

The comparison with results of other methods proves that NN are very appropriate tools to predict the EOPs. It should be pointed out that it is essential for the prediction accuracy to stop the training of the net at the right moment because the prediction error increases

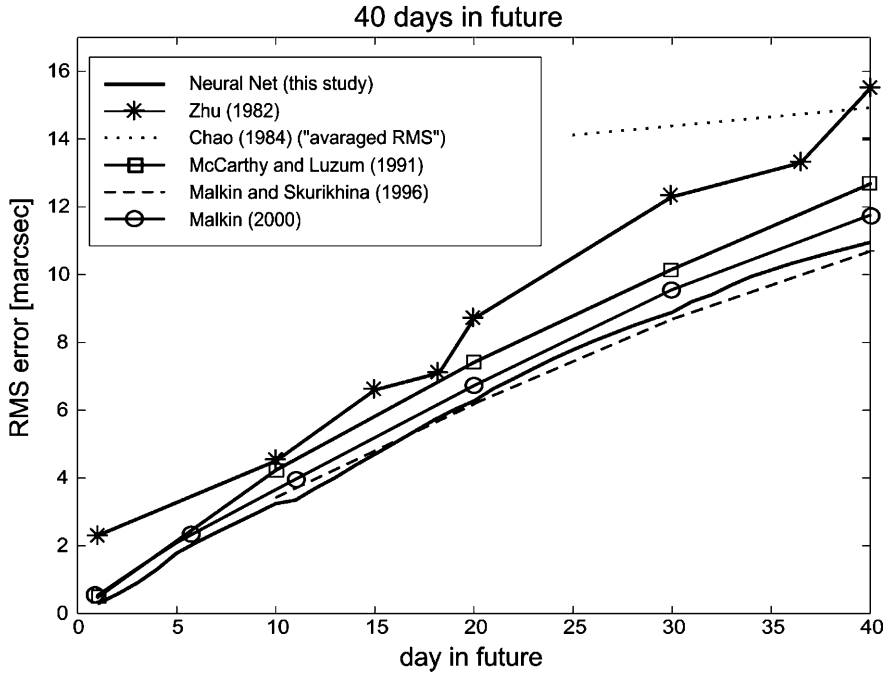


**Fig. 14.** RMS error of short-term prediction (up to 40 days) of polar motion

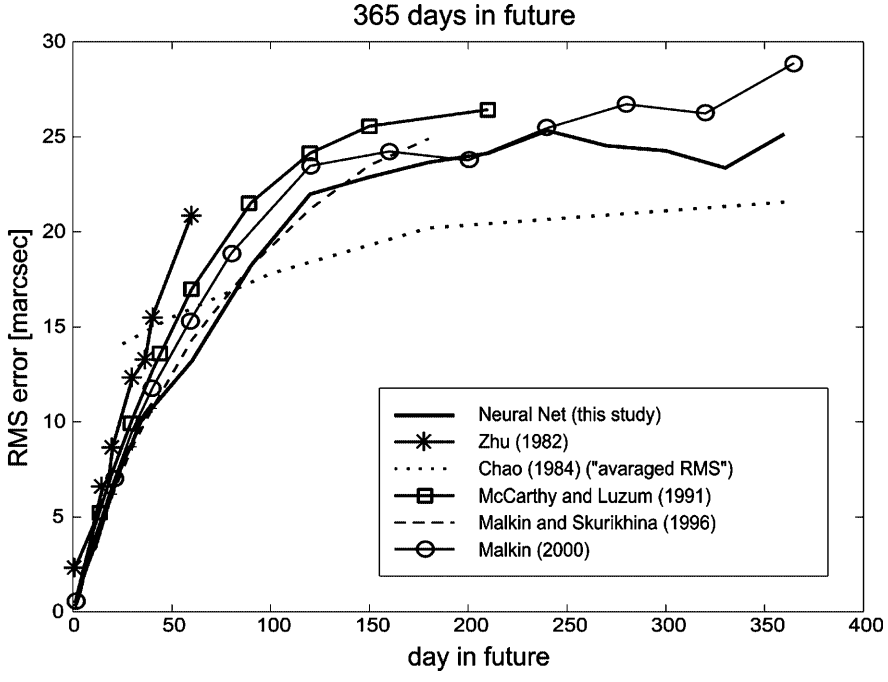


**Fig. 15.** RMS error of mean-term prediction (up to 1 year) of polar motion

rapidly after reaching its minimum. Sometimes it might become a problem to hit the exact minimum.

Despite the good quality of predictions obtained so far, further improvements are possible as follows.

Additional a priori information entered into the network may increase the accuracy, mainly of short-term prediction.

The atmospheric angular momentum (AAM) predictions of LOD are issued in advance of real time and could support EOP prediction as additional input information. These AAM-based LOD predictions could be entered into the artificial neural net as pseudo-observational data, similar to what is done in some other systems.

The inclusion of GPS results of EOPs, which are much more rapidly available than the results of any other technique, can also improve the short-term prediction.

A priori variable smoothing of the observed data, depending on the prediction length, could improve mean-term and long-term predictions.

The different accuracies of the observed EOPs over recent years have not been considered in our study. This

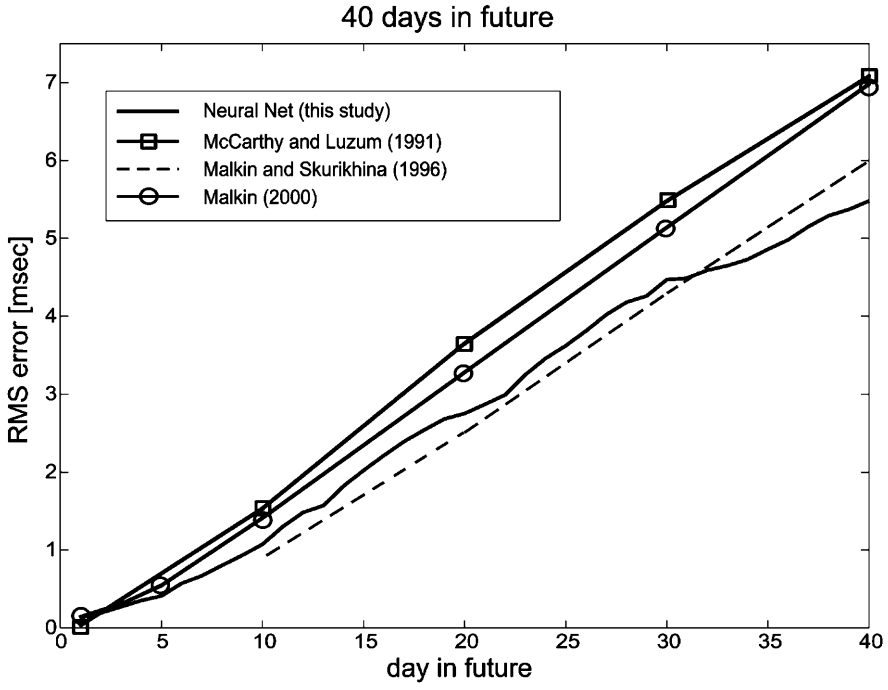


**Fig. 16.** RMS error of short-term prediction (up to 40 days) of UT1–UTC

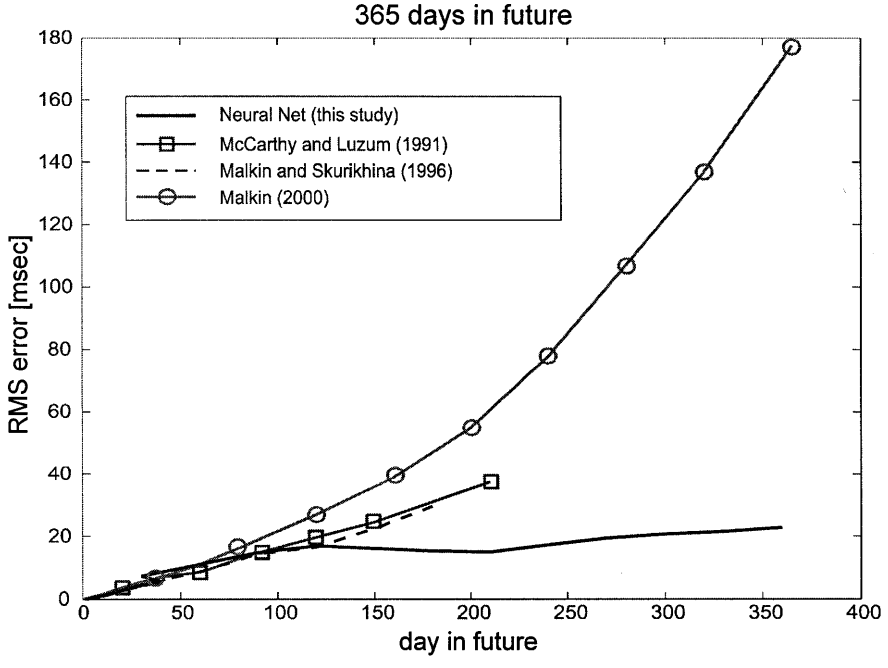


**Fig. 17.** RMS error of mean-term prediction (up to 1 year) of UT1–UTC

could be done by weighting the training data according to the increasing accuracy of EOP observations in recent years. Older data should then be trained with less iterations than data from recent years.

## References

Chao BF (1984) Predictability of the Earth's polar motion. Bull Géod 59: 81–93

Conway AJ (1998) Time series, neural networks and the future of the Sun. Department of Physics and Astronomy, University of Glasgow

Cybenko G (1989) Mathematics of control, signal and systems.

Egger D (1992) Neuronales Netz prädiziert Erdrotationsparameter. Allg Vermess Nachr 11/12: 517–524

Egger D, Fröhlich H (1993) Prädiktion von Erdrotationsdaten – klassisch und neuronal. Allg Vermess Nachr 10: 366–375

Freedman AP, Steppe JA, Dickey JO, Eubanks TM, Sung LY (1994) The short-term prediction of universal time and length of day using atmospheric angular momentum. J Geophys Res, 99(B4): 6981–6996

Malkin Z (2000) On estimation of real accuracy of EOP prediction. In: Dick S, McCarthy D, Luzum B (eds) Polar motion: historical and scientific problems, IAU Colloquium 187, Cagliari, September 1999. Astron Soc Pac, San Francisco 208: 505–510

Malkin Z, Skurikhina E (1996) On prediction of EOP. Comm IAA 93
McCarthy DD (ed) (1996) IERS tech note 21, IERS conventions, Observatoire de Paris, Paris
McCarthy DD, Luzum BJ (1991) Prediction of Earth orientation. Bull Géod 65: 18–22
Ulrich M (2000) Vorhersage der Erdrotationsparameter mit Hilfe Neuronaler Netze. IAPG/FESG no. 9, Institut für Astronomische und Physikalische Geodäsie, Technische Universität München, München
Vondrák J (1999) Earth rotation parameters 1899.7–1992.0 after re-analysis within the HIPPARCOS frame. Surv Geophys 20: 169–195
Yoder CF, Williams JG, Parke ME (1995) Tidal variations of Earth rotation. J Geophys Res 86(B2): 881–891
Zell A (1994) Simulation Neuronaler Netze. Addison-Wesley, Reading, MA
Zell A, Mamier G, Vogt M, Mache N, Hübner R, Döring S, Herrmann KU, Soyez T, Schmalzl M, Sommer T, Hatzigeorgiou A, Posselt D, Schreiner T, Kett B, Clemente G, Wieland J (1995) SNNS, Stuttgart Neural Network Simulator, User Manual, Version 4.1
Zhu SY (1981) Prediction of Earth rotation and polar motion. Rep 320 Department of Geodetic Science and Surveying, The Ohio State University, Columbus
Zhu SY (1982) Prediction of polar motion. Bull Géod 56: 258–273